J Nanostruct 7(2): 147-154, Spring 2017

RESEARCH PAPER

A Comparative Study of the Synthesis and Thermal Stability of Nanostrucrured Al and Al-Mg Powders Fabricated by Mechanical Alloying Technique

Seyyed Amin Rounaghi [1]* *and Elaheh Esmaeili* [2]

[1] *Department of Materials Engineering, Birjand University of Technology, Birjand, Iran*

[2] *Department of Chemical Engineering, Birjand University of Technology, Birjand, Iran*

ARTICLE INFO

Article History:
Received 10 January 2017
Accepted 12 March 2017
Published 01 April 2017

Keywords:
Aluminum
Heating
Magnesium
Milling
Nanostructured powders

ABSTRACT

Nanostructured Al and Al-Mg (Mg 30 wt. %) powders with the mean crystallite sizes of 42 and 11 nm were prepared through the solid state ball milling technique. The milling process was performed for various times up to 12 h in argon atmosphere and the synthesized powders were in detail characterized by different techniques. The effect of milling time and Mg addition on the size, morphology, chemical composition, phase structure and crystallite size of the powder particles were thoroughly investigated and the results were compared with the non-alloyed Al system. Two distinct particle morphologies comprising lamellar flakes and solid granules were obtained as final milling products in Al and Al-Mg systems, respectively. It was revealed that Mg atoms gradually diffuse into the Al lattice during milling and form a supersaturated Al-Mg solid solution (α phase). Thermal analyses of the powders revealed that metastable nanostructures formed during the milling transform into the equilibrium and stable phases such as Al_4C_3 and Al_2Mg_3 (β) upon the heating.

How to cite this article
Rounaghi S. A, Esmaeil E. A Comparative Study of the Synthesis and Thermal Stability of Nanostrucrured Al and Al-Mg Powders Fabricated by Mechanical Alloying Technique. J Nanostruct, 2017; 7(2):147-154. DOI: 10.22052/jns.2017.02.009

INTRODUCTION

Nano-size and nanostructured aluminum-based powders have attracted great interest and revolutionized many key areas of science and technology. The main applications of aluminium-based compounds include their utilization as energetic materials in pollutant and explosive industries [1], plasmonic metamaterials in optics-based technologies [2], precursor in thermite reactions [1] and hydrogen producer in fuel cells [3]. Moreover, nanoscale Al (n-Al) powder has been widely studied for production of high strength alloys and composites with potential applications in automobile and aerospace industries [4].

The methods for the manufacturing of n-Al are basically divided into three distinct categories, including vapor phase condensation, liquid phase chemistry and solid state reaction [1, 5, 6].

N-Al fabrication by the solid state metathesis is more attractive because of no demand for any solvents. The energy of reaction, in this route, is usually provided by either heat treatment or mechanical forces (or both of them, so called "Mechanothermal"). Mechanical milling is the most frequently technique used for room temperature solid state synthesis of nanoparticles through the energy of ball impacts. N-Al powder is fabricated by milling process through either the breakdown of large Al particles (top-down) [5, 6] or implementation of a chemical reaction (bottom-

* *Corresponding Author Email: rounaghi@birjandut.ac.ir*

up) [7]. The top-down approach, however, is more favorable due to the low-cost reactants and commercially-available aluminum powder. During this process, the soft Al particles are frequently deformed, fractured and cold welded under severe ball impacts, causing the formation of ultra-fine Al particles with nano-crystalline structure [5]. Since, the final size of particles is usually critical, a balance between fracturing and cold welding processes is required. In most cases, a suitable processing control agent (PCA) is used to impede the cold welding of particles. For instance, various compounds such as hexane, iodoform and stearic acid have been successfully employed for the reduction of particles size during the milling process [5, 8].

Recently, it has been demonstrated that the size, structure and properties of elemental Al powder can be significantly improved by alloying. Milling, in this case, is referred to the conventional mechanical alloying process in which the Al powder is mechanically alloyed with the other elements such as Mg [9], Ti [10], Cu [11] and Fe [12]. Among them, the mechanically alloyed Al-Mg has attracted much more attention due to the potential applications in metallic fuels, propellants and pyrotechnics [1]. It has been reported that the milling process extends the solid solubility of Mg in Al and forms nanosize structures and metastable intermetallic phases which in turn, enhances the mechanical properties and the reactivity of products [9].

Herein, we report a novel comparative study on the effect of the ball milling process on the phase evolution, structure, size, morphology and thermal stability of the metallic powders in both Al and Al-Mg powder systems. Moreover, the role of magnesium addition on the structural evolutions and material developments is rationalized.

MATERIALS AND METHODS

Al (purity > 99.5 wt. %) and Mg (purity > 99.8 wt. %) powders were purchased from Mashhad Powder Metallurgy Co. and Alfa Aesar Co., respectively. Aluminum samples were prepared in the absence and/or the presence of magnesium denoted as Al and Al-30Mg (Mg 30 wt. %) systems, respectively. In both cases, stearic acid (purity > 97 wt. %, Merck) was used as PCA and added 4 wt. % of the materials. For each experiment, 3 g of the premixed powder was introduced into a steel vial together with hardened steel balls (10 mm diameter) to give a ball to powder weight ratio of 50:1. To avoid powder oxidation, vial charging and sampling were performed inside an argon filled glove box with O_2 and H_2O contents less than 1 ppm. Milling was conducted at room temperature using a high energy planetary ball mill at a rotating speed of 300 rpm. The powders were milled for various times up to 12 h and at each time a small quantity of powder was removed and stored inside of the glove box for further characterizations.

The phase and microstructure of the powders were analyzed by a Philips X'Pert X-ray diffractometer with Co Kα radiation (λ = 0.17889 nm). The Rietveld refinement method was used to determine the crystallite size of the milled products. The powder structure was investigated using a scanning electron microscope (SEM, Tescan VEGA II LMU) operated at 20 kV and equipped with an energy dispersive X-ray spectrometer (EDX). Thermal stability of the samples was studied by a differential scanning calorimeter (DSC 404 F1 Pegasus from Netzsch) at heating rate of 20 °C/min under a continuous flow of argon.

RESULTS AND DISCUSSION

XRD analysis was performed to determine the phase evolution of powders as a function of milling time in both Al and Al-30Mg systems. As shown in Fig. 1a, milling has no obvious effect on the phase transitions in the Al system, except slight peak shifts together with the peak broadenings resulted from and the strain-induced structure with fine crystallites. Fig. 1b demonstrates the variation of the crystallite size and lattice strain of aluminum as a function of milling time. The decrease of crystallite size is along with the enhancement of the lattice strain level, when the milling time is increased. Moreover, the crystallite size exhibits an abrupt reduction at the early stages of milling, however, further refinement proceeds slowly, such that the grain size finally reaches to a steady-state value of 54 nm at the end of milling. This trend is resulted from the ease of dislocation mobilities followed by the formation of nano-size dislocation cells at the time range of 2-4 h, which in turn, leads to a suddenly decrease of crystallite size. When the milling time exceeds 4 h, further crystallite refinement is compensated by simultaneous dynamic recovery and recrystallization, leading to the stabilization of the crystallite size. Conversely, the lattice strain is relatively small at the first stages of milling due

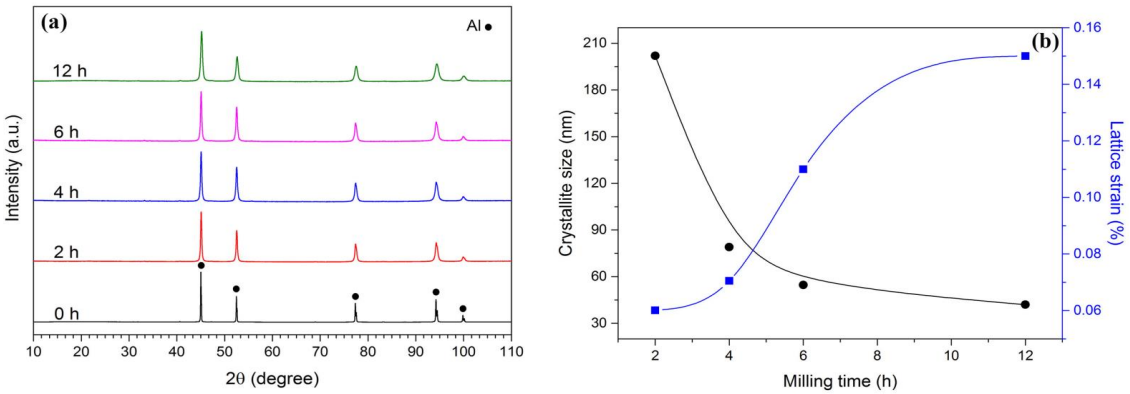

Fig. 1. a) XRD patterns and b) crystallite size versus lattice strain of the Al powder milled for various times.

to the ease of dislocation movements and rapidly increases at the prolonged milling times, when dislocation mobilities are effectively suppressed due to the interaction with intragranular obstacles and grain boundaries. Further deformation in this step is mainly governed by the grain-boundary sliding, leading the lattice strain reaches a constant value [13].

Fig. 2 illustrates phase evolutions in Al-30Mg system during milling. The pattern of as-blended powder (0 h) reveals two series of distinct peaks corresponding to the elemental Al and Mg. The intensity of Mg peaks gradually decreases when milling progresses and entirely disappears after 6 h. Meanwhile, weak and broad peaks corresponding to the α-Al phase appear which are inferred to the diffusion of Mg into the Al crystal structure and fabrication of the Al-Mg solid solution. This structural phase exhibits a strong inhomogeneity at the milling times shorter than 6 h (the asymmetry of α peaks in the patterns), but, it improves, when the milling time exceeds 12 h. The XRD pattern of materials obtained at the final stages of the milling presents broad peaks indexed to the nanostructured α phase with a mean crystallite size of 11 nm. The measured lattice strain for this sample (12 h) results in a value of 0.35 % which is significantly higher than that of obtained for the Al system. The small crystallite size and high lattice strain measured for the Al-30Mg system are attributed to the formation of α phase which suppresses dislocation mobilities by the solid solution strengthening mechanism [14]. In this case, dislocation pinning at the solute

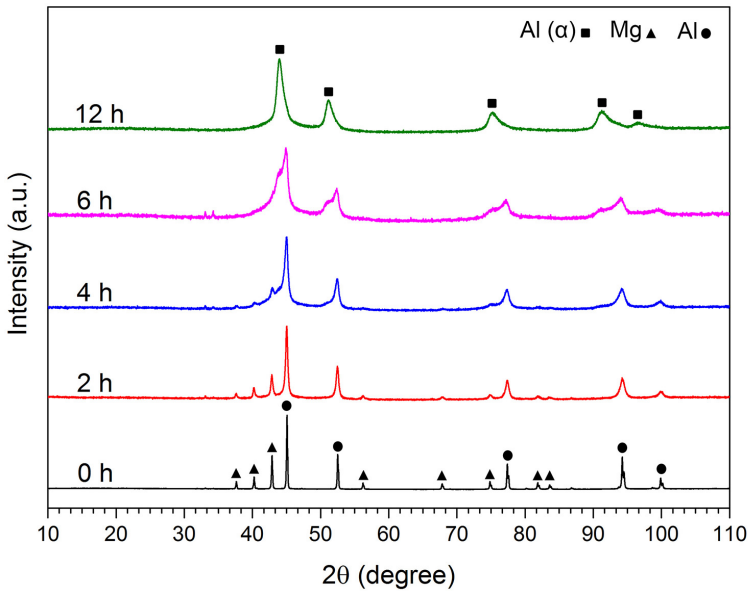

Fig. 2. XRD patterns of the Al-30Mg powder milled for various times.

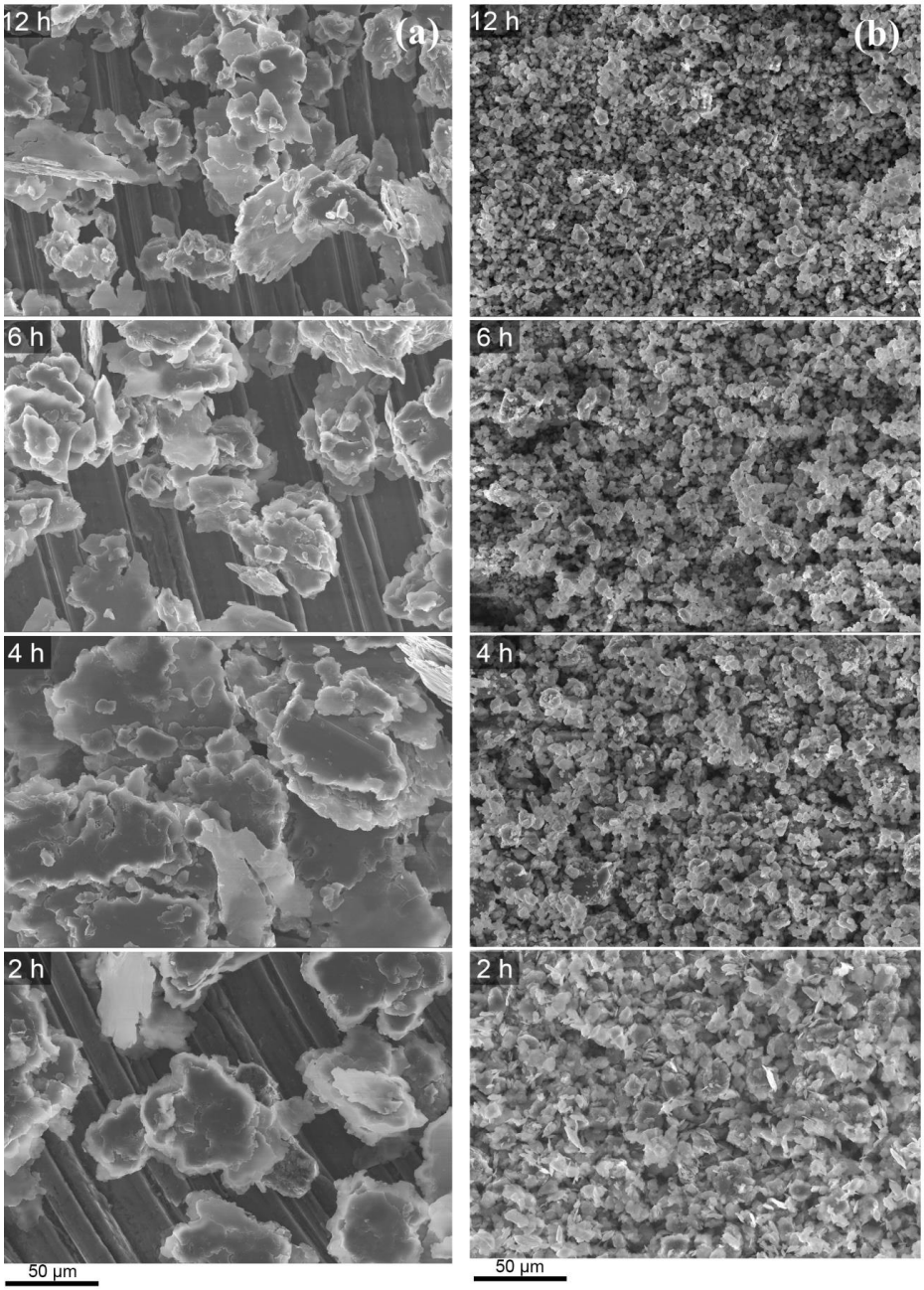

Fig. 3. a) SEM images of the powder particles milled for various times. a) Al and b) Al-30Mg milling systems.

Mg atoms not only enhances the lattice strain by reduction of deformability but also reduces the crystallite size through the enhancement of dislocation density and the formation of subgrain boundaries.

Based on the XRD analyses, there is no evidence related to the possible formation of Al_2Mg_3 (β) phase even at the long milling times up to 12 h. The absence of β phase in our results should be addressed to its complex crystal structure with a giant unit cell containing about 1168 atoms which requires a long range diffusion of Al and Mg atoms to nucleate [15]. Although the β phase is thermodynamically more stable [16], but the formation of metastable α phase appears to be kinetically easier because of the simple crystal structure.

The morphological evolution of the powders

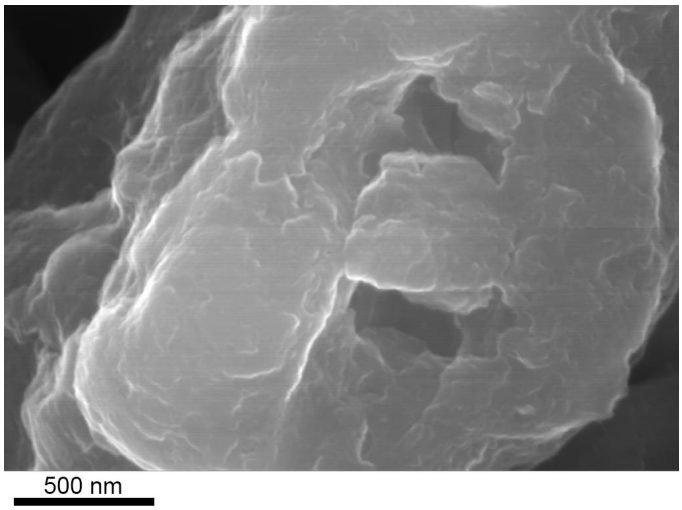

Fig. 4. A typical SEM image of a powder particle in Al-30Mg system milled for 12 h.

at various milling times is investigated by SEM technique for both Al and Al-30Mg systems, as shown in Fig. 3. Under the aggressive mechanical forces, the ductile Al particles easily deform to the flakes after 2 h milling (Fig. 3a). The particle morphology, although, remains relatively constant up to the end of milling (12 h), but the size of flakes gradually decreases as a function of milling time. It is worthy to note that the strength of materials is increased during the milling through the activation of various mechanisms such as strain hardening, grain refinement and solid solution strengthening [14]. The strength enhancement, however, is usually accompanied by the increasing of the brittleness which facilitates the fracture of particles and the powder refinement during the process.

The SEM observations conducted on the Al-30Mg alloying system demonstrate a quite different trajectory (Fig. 3b). The flake-shaped particles, in this case, are formed at the early stages of milling and gradually transform to the plump granules by further milling. To justify this trend, the microstructure and phase evolutions of the powder at each period of the milling time should be taken into consideration. As previously shown, the Al-Mg solid solution (α phase) is formed, when the milling exceeds 2 h (Fig. 2). Hence, the deformation mechanism and particle morphology at the prior of this time (< 2 h) should be similar to that of pure Al (flake-shaped particles). When the milling time exceeds 2 h, the ductility of Al particles reduces dramatically, due to the diffusion of Mg atoms and the formation of α phase. The structural brittleness makes the flake particles susceptible for the fracture which in turn, leads to the formation of fine plump

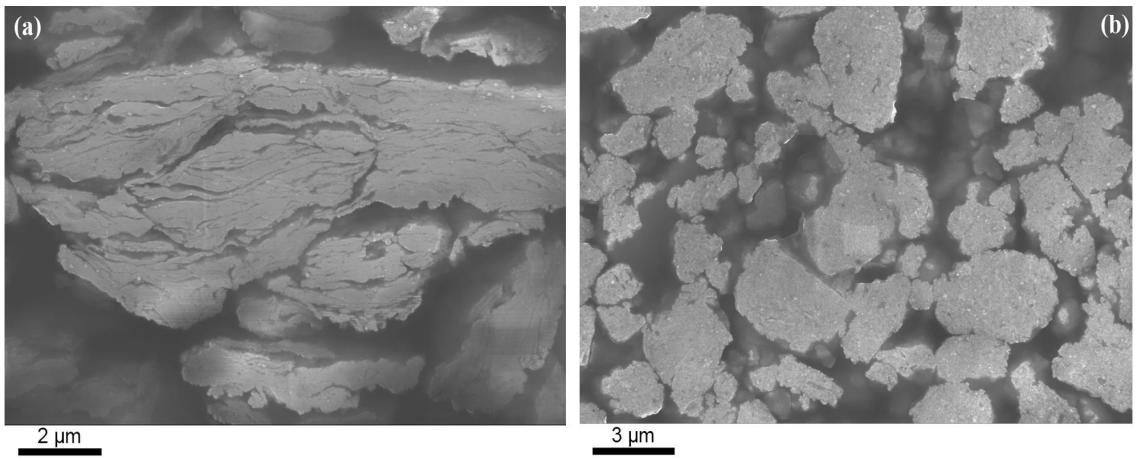

Fig. 5. Typical cross-sectional SEM images of the Al-30Mg powder particles milled for a) 2 h and b) 12 h.

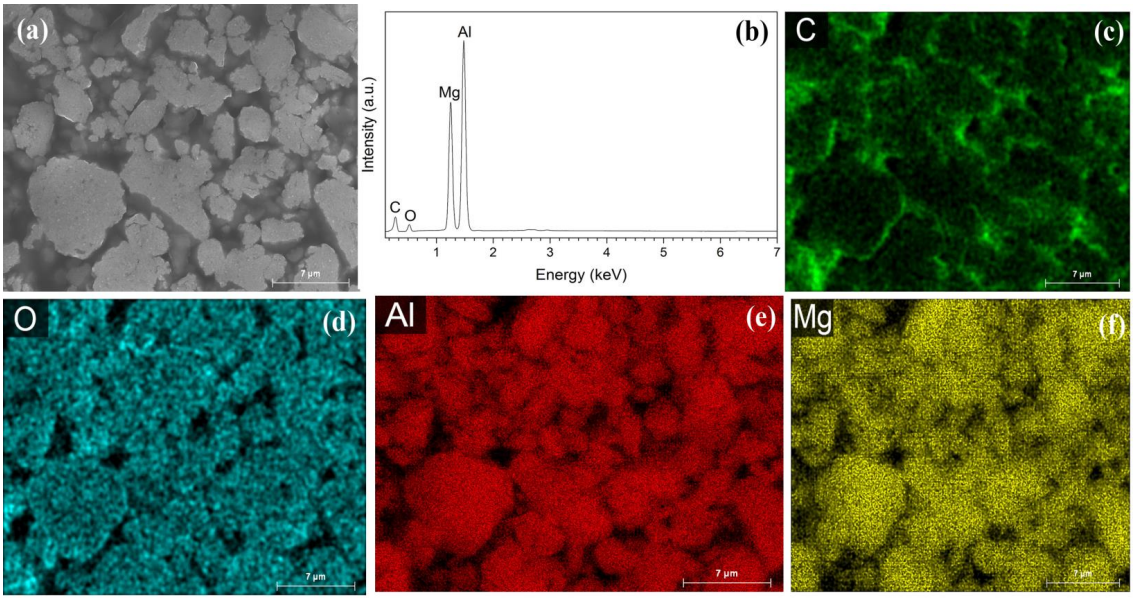

Fig. 6. a) Typical cross-sectional SEM image of 12 h milled Al–30 Mg powder. b) Corresponding EDX spectrum and c-f) elemental map analysis.

granules at the prolonged milling times (12 h). High magnification SEM images taken from the fabricated granules reveal that the surface is structured in the nanometer scales (Fig. 4), which is in accordance with Rietveld refinement analysis.

The cross-sectional SEM images obtained from the Mg alloyed samples milled for 2 h and 12 h demonstrate two distinctive structures with different particle-packing density; i.e. lamellar flakes and solid granules, respectively (Figs. 5a and b). According to Fig. 5a, the highly distorted structure of the Al particles milled for 2 h implies the severe plastic deformation induced by the ball milling process. This lamellar structure turns into the solid granules, when the ductility reduces due to the fabrication of Al-Mg solid solution at the prolonged milling times (Fig. 5b).

A typical cross-sectional SEM image of 12 h milled Al–30 Mg powder is provided in Fig. 6a. The corresponding EDX spectrum illustrates that the chemical structure is consisted of the elemental aluminum, magnesium, oxygen and carbon (Fig. 6b). The origin of the carbon peak arises from the graphite filler and the organic resin used for the mounting of the sample which is in a good agreement with carbon map (Fig. 6c). The appearance of weak oxygen peak along with the corresponding O map (Fig. 6d) is attributed to the surface oxidation of the particles during sample handling and preparation. The EDX maps of Al and Mg (Figs. 6e and f) demonstrate a uniform distribution of these metallic elements inside of the powder particles. This is in consistent with the previous results which confirms the formation of the Al-Mg solid solution and implies to the absence of the intact Mg in the final products.

The results of the thermal stability of the milled Al and Al-30Mg powders together with the as-blended Al (Al-4 wt. % PCA) are illustrated in Fig. 7. The DSC scans of both the as-blended and the milled Al present a strong endothermic peak at 665 °C and 658 °C, respectively, which is attributed to the melting of aluminum (Figs. 7a and b). The higher intensity and the slight shift towards lower temperatures observed for the milled sample is attributed to the solution of impurities as well as the formation of nanostructured Al [17]. The stored mechanical energy in the sample during milling is another possible reason for the lowering of T_m which is also deduced from the negative background observed in the DSC scans of the milled products (Figs. 7b and c). In the DSC curve of the milled Al (Fig. 7b), the broad exothermic peak centroid at 400 °C is associated with the formation of Al_4C_3, as confirmed by the corresponding XRD pattern of this sample obtained after the heat treatment (Fig. 8a). The origin of carbon atoms in Al_4C_3 comes from stearic acid used as organic PCA. From Fig. 7c, the DSC scan of the milled Al-30Mg powder, shows a different trend compared to

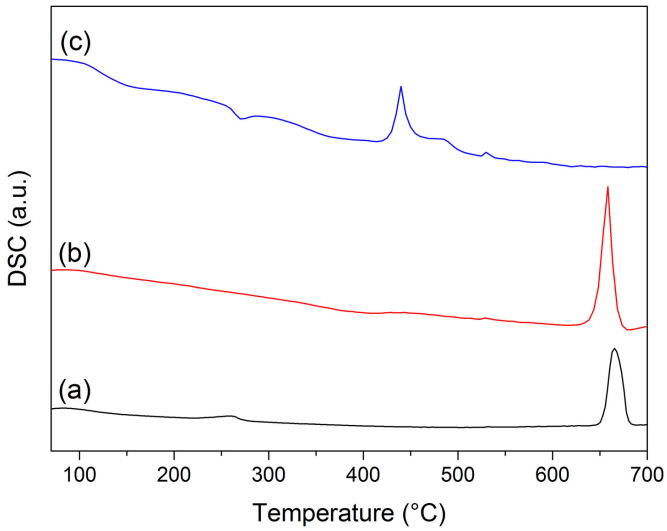

Fig. 7. DSC scans of a) as-blended Al and 12 h milled b) Al and c) Al-30Mg systems in argon.

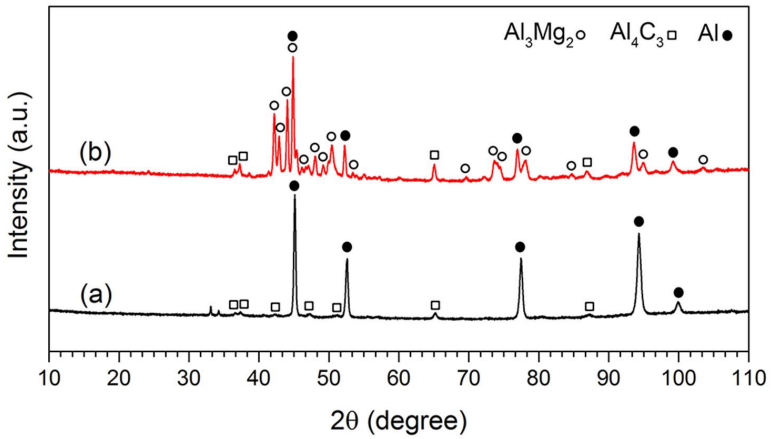

Fig. 8. XRD patterns of 12 h milled a) Al and b) Al-30Mg powder systems after heating to 700 °C in argon.

the unalloyed systems. The corresponding curve displays three distinct exothermic peaks and one broad endothermic peak upon the heating up to 700 °C. The first exothermic transition observed at about 169 °C is assigned to the formation of $Al_{12}Mg_{17}$ intermetallic phase (γ) [9]. This phase is not thermodynamically stable with respect to the equilibrium Al-30Mg phase diagram, hence, it transforms to much more stable phases by further heating. This confirms the absence of γ peaks in the XRD pattern of the heat-treated products (Fig. 8b). The second exothermic peak at around 270 °C is associated with the formation of as a hexagonal phase with the composition of Al_3Mg_2 [9]. This phase serves as the precursor for the formation of the β phase by further heating, as corroborated by the corresponding peaks in the XRD pattern (Fig. 8b). In fact, the applied thermal treatment process provides enough time and energy for atomic rearrangements and long-range diffusion of Al and Mg atoms which are crucial for the formation of a complex structure like β phase. The third exothermic peak at 364 °C is assigned to the formation of Al_4C_3 which confirms by the XRD result (Fig. 8b). The multiple endothermic peaks in the temperature range of 410 °C to 540 °C with a major at 439 °C are attributed to the melting of α and β phases, which indicates an obvious reduction in the melting point of the powder. The onset temperature of the major endothermic peak at 428 °C is lower than the reported equilibrium melting temperature of 450 °C for Al-30Mg alloying

system [16]. This is explained by the nanostructure characteristics of the phases formed during both the milling and heating processes. The extended melting temperature of the powder is also justified by the high heating rate applied as well as the inhomogeneity of the synthesized powder in good accordance with the asymmetry of the α phase in the XRD patterns.

CONCLUSIONS

Mechanical alloying was employed to fabricate nanostructured Al and Al-Mg powders. Due to the milling impacts, Mg atoms progressively diffuse into the Al and form a uniform supersaturated Al-Mg structure. Two distinct types of particles comprising the lamellar flakes and solid granules were obtained by the long milling of the Al and Al-30Mg systems, respectively. The particle size, in both systems, revealed a significant reduction as a function of milling time which was attributed to the structural brittleness caused by work hardening. Moreover, the particle size refinement was drastically higher in the Mg alloyed system due to the simultaneous activation of the two strengthening mechanisms, i.e. work hardening and solid solution strengthening. Post thermal treatment of the milled powders resulted in the formation of two Al_4C_3 and Al_2Mg_3 (β) intermetallics. The results revealed that Al_2Mg_3 (β) with the complex structure forms only during the post heat treatment process which provides the required energy and time for the atomic rearrangements and long-range diffusion of Mg and Al atoms.

CONFLICT OF INTEREST

The authors declare that there are no conflicts of interest regarding the publication of this manuscript.

REFERENCES

1. Dreizin EL. Metal-based reactive nanomaterials. Prog. Energy Combust. Sci. 2009;35(2):141-67.
2. Knight MW, King NS, Liu L, Everitt HO, Nordlander P, Halas NJ. Aluminum for Plasmonics. ACS Nano. 2014;8(1):834-40.
3. Shimamura K, Shimojo F, Kalia RK, Nakano A, Nomura K-i, Vashishta P. Hydrogen-on-Demand Using Metallic Alloy Nanoparticles in Water. Nano Lett. 2014;14(7):4090-6.
4. Khan AS, Suh YS, Chen X, Takacs L, Zhang H. Nanocrystalline aluminum and iron: Mechanical behavior at quasi-static and high strain rates, and constitutive modeling. Int. J. Plast. 2006;22(2):195-209.
5. Khorasani S, Abdizadeh H, Heshmati-Manesh S. Evaluation of structure and morphology of aluminum powder particles milled at different conditions. Adv. Powder Technol. 2014;25(2):599-603.
6. McMahon BW, Yu J, Boatz JA, Anderson SL. Rapid Aluminum Nanoparticle Production by Milling in NH_3 and CH_3NH_2 Atmospheres: An Experimental and Theoretical Study. ACS Appl. Mater. Interfaces. 2015;7(29):16101-16.
7. Paskevicius M, Webb J, Pitt MP, Blach TP, Hauback BC, Gray EM, et al. Mechanochemical synthesis of aluminium nanoparticles and their deuterium sorption properties to 2 kbar. J. Alloys Compd. 2009;481(1–2):595-9.
8. Abraham A, Zhang S, Aly Y, Schoenitz M, Dreizin EL. Aluminum–Iodoform Composite Reactive Material. Adv Eng Mater. 2014;16(7):909-17.
9. Scudino S, Sakaliyska M, Surreddi KB, Eckert J. Mechanical alloying and milling of Al–Mg alloys. J. Alloys Compd. 2009;483(1–2):2-7.
10. Al-Dabbagh J, Tahar R, Ishak M, Harun S. Synthesis and Characterization of Nano Ti-50%Al by Mechanical Alloying. In: Öchsner A, Altenbach H, editors. Design and Computation of Modern Engineering Materials. Advanced Structured Materials: Springer International Publishing; 2014. p. 329-43.
11. Kong Q, Lian L, Liu Y, Zhang J. Fabrication and Characterization of Nanocrystalline Al–Cu Alloy by Spark Plasma Sintering. Mater. Manuf. Processes. 2014;29(10):1232-6.
12. Archana MS, Ramakrishna M, Gundakaram RC, Srikanth VVSS, Joshi SV, Joardar J. Nanocrystalline Phases During Mechanically Activated Processing of an Iron (Fe) Aluminum (40 at% Al) Alloy. Mater. Manuf. Processes. 2014;29(7):864-9.
13. Wei YJ, Anand L. Grain-boundary sliding and separation in polycrystalline metals: application to nanocrystalline fcc metals. J Mech Phys Solids. 2004;52(11):2587-616.
14. Ma K, Wen H, Hu T, Topping TD, Isheim D, Seidman DN, et al. Mechanical behavior and strengthening mechanisms in ultrafine grain precipitation-strengthened aluminum alloy. Acta Mater. 2014;62:141-55.
15. Scudino S, Sperling S, Sakaliyska M, Thomas C, Feuerbacher M, Kim KB, et al. Phase transformations in mechanically milled and annealed single-phase β-Al_3Mg_2. Acta Mater. 2008;56(5):1136-43.
16. Kulkarni K, Luo A. Interdiffusion and Phase Growth Kinetics in Magnesium-Aluminum Binary System. J Phase Equilib Diffus. 2013;34(2):104-15.
17. Puri P, Yang V. Effect of Particle Size on Melting of Aluminum at Nano Scales. J. Phys. Chem. C. 2007;111(32):11776-83.